Journal of South American Earth Sciences xxx (2010) xxx–xxx

Contents lists available at ScienceDirect

Journal of South American Earth Sciences

journal homepage: www.elsevier.com/locate/jsames

Volcanic evolution of the back-arc Pleistocene Payun Matru volcanic field (Argentina)

A. Germa [a,*], X. Quidelleur [a], P.Y. Gillot [a], P. Tchilinguirian [b]

[a] UMR CNRS 8148 IDES, Département des Sciences de la Terre, Equipe de Géochronologie et Volcanologie, Bat. 504, Université Paris-Sud 11, 91405 Orsay Cedex, France
[b] SEGEMAR, Universidad de Buenos Aires, Buenos Aires, Argentina

ARTICLE INFO

Article history:
Received 26 June 2008
Accepted 21 January 2010
Available online xxxx

Keywords:
Andes
Payun Matru
Back-arc volcanism
Caldera
K–Ar dating
Pleistocene

ABSTRACT

For the first time, about 30 volcanic formations of the back-arc Payun Matru volcanic field (Payun Matru volcanic field, Argentina, 36°S, 69°W) have been sampled for K–Ar geochronology and geochemistry in order to reconstruct the eruptive history of this key province in the Andean back-arc. The Payun Matru volcanic field has been built since final Pleistocene until present with ages ranging from 280 ± 5 to 7 ± 1 ka. Erupted lavas belong to calc-alkaline series, with characteristics of both arc and intraplate magmas. From previous studies, three main units are distinguished: (1) a basaltic field (Los Volcanes), which covers a large surface of the Payun Matru volcanic field, composed of strombolian cones and associated lava flows emitted from 300 ka to Holocene times, (2) the stratovolcano Payun, with intermediate compositions, built around 265 ka, and (3) the shield volcano Payun Matru s.s. characterized by trachytic compositions and a large summit caldera. The earlier stages of the Payun Matru volcano are not dated, but we constrain the major explosive event, related to the eruption of a widespread ignimbrite and to the formation of the caldera, between 168 ± 4 ka (internal wall of caldera) and 82 ± 1 ka (flow within the caldera). Based on the geochemical similarities of the ignimbrite and the upper lava flow of the pre-caldera cone, we suggest that the age of this event is most probably at the older end of this interval. Numerical modeling using a GIS program has been used to reconstruct the morphological evolution for Payun Matru volcano before and after the caldera collapse. The ancient edifice could be modeled as a flattened cone, 2300 m high, with a volume of about 240 km^3. The ignimbrite eruption associated with the Payun Matru caldera formation could be related to the regional tectonic environment, which is characterized by multiple Plio-Pleistocene extensional stages during the last 5 Myr. The evolution of the Nazca plate subduction from a flat slab to a normal dip induced an input of fluid mobile elements and asthenosphere plume-like mantle source beneath the Patagonian lithosphere, which yields the observed intraplate signature. We also interpret this geodynamic evolution as the influence of extensive processes in the upper crust leading to caldera-forming eruptions as observed throughout this province.

© 2010 Elsevier Ltd. All rights reserved.

1. Introduction

The studied area is located in the north of the Andean southern volcanic zone (SVZ; 33°30′S–46°30′S), a 1000-km-long volcanic chain (Fig. 1). One of the interests of the studied region lies in the relationship between the wide ranges of back-arc volcanic products in this particular location of the SVZ, where several successive stages of flat to normal subduction have been recognized (Kay et al., 2006). Recently, studies have been focused on the surrounding zone to characterize the back-arc basaltic volcanism at this latitude (Bermudez et al., 1993; Delpino, 1993; Inbar and Risso, 2001a,b; Risso et al., 2008) but less attention has been paid to evolved rocks and andesitic volcanoes. The aim of the present study is to provide a time constrained geochemical dataset in order to widen out investigations to evolved rocks and to reconstruct the volcanic history of the Payun Matru volcanic field (Payun Matru volcanic field). In this paper, we first present the geochronological data (K–Ar dating) obtained on 14 samples from the whole complex. Then, we describe the geochemical data for 31 representative samples. Finally, a morphological study (DEM) of the Payun Matru volcanic field is used to complete our interpretations.

2. Geological setting

2.1. Regional setting

The Payun Matru volcanic field (from 36°10′S to 36°35′S) belongs to the back-arc volcanism of the Andean range in Argentina, at about 530 km east of the Nazca plate subduction trench (Fig. 1).

* Corresponding author. Tel.: +33 1 69 15 53 54.
E-mail address: aurelie.germa@u-psud.fr (A. Germa).

0895-9811/$ - see front matter © 2010 Elsevier Ltd. All rights reserved.
doi:10.1016/j.jsames.2010.01.002

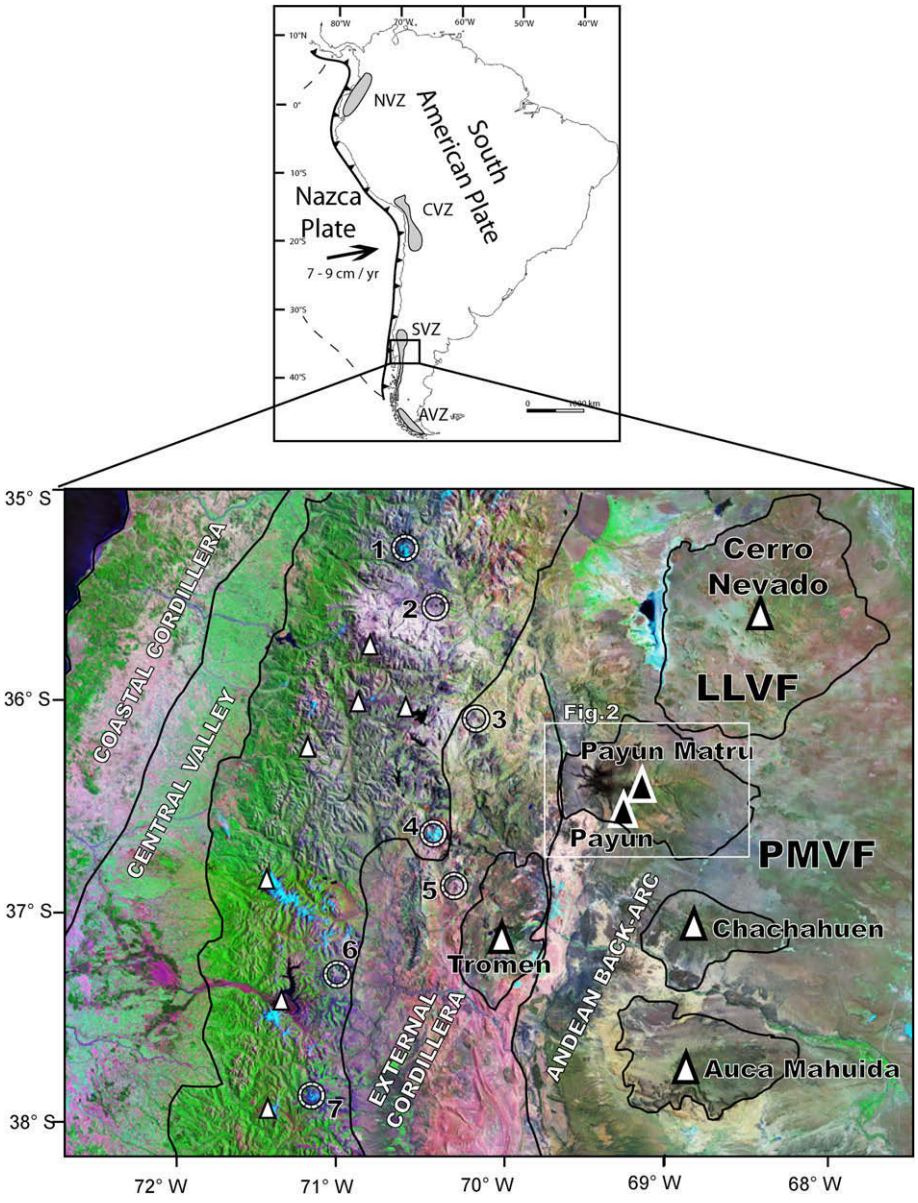

Fig. 1. Map of the Andean subduction-zone system showing the general tectonic setting and distribution of active volcanic zones (NVZ, CVZ, SVZ and AVZ). Arrow indicates the direction of the Nazca plate motion relative to the South American plate (Gripp and Gordon, 2002). Below, satellite image (LANDSAT 7) of the studied area, showing the back-arc location of the Llancanello volcanic field (LLVF) and Payun Matru volcanic field (PMVF). Main volcanoes are located with white triangles. Plio-Pleistocene calderas are located with black-and-white circles: (1) Planchon-Azufre, (2) Calabozos, (3) Bobadilla, (4) Domuyo, (5) Palao, (6) Trohunco and (7) Copahue.

In the area investigated here, to the northern end of the SVZ (33–39°S), Quaternary volcanism is identified as both arc volcanism in the principal cordillera and back-arc volcanism in the Mendoza–Neuquén province due to periods of flat subduction during the Miocene (Kay et al., 2006; Ramos and Kay, 2006). The steepening of the slab to the present geometry since 5 Ma caused westward migration of the arc volcanism at the present active front location, and induced hot asthenosphere upwelling, implying mantle plume-like dynamics beneath the Patagonian lithosphere and preferential melting of hydrated mantle (James and Sacks, 1999; Kay et al., 2004; Ramos and Folguera, 2005). This was followed by occurrence of extensional faults which could be the cause of the formation of large quaternary collapse calderas in the Neuquén Andes to the east of the forearc (Fig. 1): Planchon-Azufre (35°15′S, 70°33′W; <0.55 Ma), Calabozos (35°33′S, 70°30′W; 0.8–0.15 Ma), Bobadilla (36°00′S, 70°30′W; 0.3 Ma), Domuyo (36°34′S, 70°25′W; 2.5 Ma), Palao Caldera (36°52′S, 70°19′W; 5–3 Ma), Trohunco (37°18′S, 71°01′W; 3.2 Ma), Copahue (37°51′S, 71°09′W; 4–2.6 Ma), Pino Hachado volcanic complex (38°40′S, 70°53′W; 5–1.4 Ma), Caldera del Agrio (37°40′S, 71°00′W; 2.5–0.8 Ma), among others (Folguera et al., 2005; Kay, 2005; Kay et al., 2004, 2005, 2006; Kay and Mpodozis, 2002; Munoz et al., 2000; Ramos and Kay, 2006; Stern et al., 1990).

The back-arc region at this latitude (Fig. 1) is characterized by the Andino-Cuyana Basaltic Province which is constituted of two main Plio-Quaternary volcanic fields covering 15,900 km^2: the Llancanelo volcanic field (1.9–0.9 Ma, Quidelleur et al., 2009) to the northeast, and the Payun Matru volcanic field to the south, also called Payenia (Bermudez et al., 1993; Bertotto et al., 2006; Ramos and Kay, 2006). They display a wide range of magmatic compositions from basalts to andesites, with the presence of isolated andesitic volcanic centers, Payun Matru and Cerro Nevado (Delpino, 1993). Numerous basaltic lava fields, composed of hundreds of effusive monogenic centers of Pleistocene and Holocene age

Please cite this article in press as: Germa, A., et al. Volcanic evolution of the back-arc Pleistocene Payun Matru volcanic field (Argentina). J. S. Am. Earth Sci. (2010), doi:10.1016/j.jsames.2010.01.002

(Inbar and Risso, 2001b), which are lined up with normal faults and fractures, are also present. With about 800 parasitic cinder cones, the Andino-Cuyana Basaltic Province has the highest number of monogenetic volcanoes in South America (Bertotto et al., 2006; Inbar and Risso, 2001b; Risso et al., 2008), and basaltic lava flows can be extremely long, e.g. the 181 km-long Pampas Onduladas flows (Pasquarè et al., 2008). Previous studies have shown that faults and fractures can be associated with extension during the Plio-Pleistocene (Arana Saavedra et al., 1984; Bertotto et al., 2006; Folguera et al., 2005; Kay, 2005; Kay et al., 2005, 2006; Ramos and Folguera, 2005; Ramos and Kay, 2006), which favor ascent of homogeneous magmas and rapid eruption over a wide area (Bermudez et al., 1993; Inbar and Risso, 2001b; Kay et al., 2005). These products have features of both back-arc alkali basalts and orogenic arc basalts, which could be linked to the melting of "wet-spot" mantle and "hot-spot" like asthenospheric conditions (Kay et al., 2004), erupted through a slab-window formed with the subduction of spreading ridges (Kay et al., 2004).

2.2. Geology of the Payun Matru volcanic field

The Payun Matru volcanic field (Fig. 2) covers an area of 5200 km^2 at a mean altitude of 2000 m above sea-level and is characterized by a vast diversity of volcanic morphologies, compositions and emitted products. The field consists of the Los Volcanes basaltic centers, with Hawaiian and Strombolian activity along east–west trending fractures, and of two evolved volcanoes, the Payun Matru Volcano, and the Payun Volcano. The Payun Matru Volcano has a large elliptical caldera 9×7 km wide, associated with an ignimbritic phase named El Portezuelo formation (Gonzales Diaz, 1972), which outcrops dominantly north and south of the volcano, and covers an area of 2200 km^2 (Gonzales Diaz, 1972). This ignimbrite emplacement, which probably resulted from the collapse of a plinian column, has been interpreted as being due to the sudden draining of the magma chamber followed by the collapse of the volcano summit. More recent trachytic lava flows and trachyandesitic lava domes (Delpino, 1993; Gonzales Diaz, 1972) were emplaced along the caldera rim, where magma ascent was made easier by fractures and faults. The highest point of the Payun Matru volcanic field is the Pleistocene 3680 m high Payun stratovolcano, located at the SW of the Payun Matru volcano (Gonzales Diaz, 1972). It is an 1800 m high cone-shaped stratovolcano with a summit crater slightly opened to the north. All flanks of the volcano are affected by erosion, with deeply incised radial canyons, suggesting that magmatic activity has now ceased.

Two basaltic fields with a total of more than 300 eruptive centers, mostly occurring along east–west-trending fissures are found in the Payun Matru volcanic field. The oldest lava flows are pahoehoe type, whereas the youngest are aa type lavas (Inbar and Risso, 2001b). West of Payun Matru Volcano is the volcanic field "Los Volcanes" with about 100 strombolian cones and associated basaltic flows forming the lava field bounded to the west by the Rio Grande River (Fig. 2). To the east of the Payun Matru volcanic field, Pleistocene to Holocene basaltic flows extending as far as 25 km from the caldera rim, as well as lapilli cones, have been related to east–west trending fractures (Gonzales Diaz, 1972). This field includes an old and a younger group named Guadaloso and El Rengo groups, respectively (Inbar and Risso, 2001b). Based on morphological studies, Inbar and Risso (2001a,b) proposed that the cones of the Guadaloso group (75% of them) are of Plio-Pleistocene age, while the cones of the El Rengo group are similar to the Lower Tromen group and Los Volcanes emplaced during the Holocene, with some eruptions less than 1 ka (Inbar and Risso, 2001b). The latter age is supported by the strikingly dark, unweathered basalt (Fig. 2) and local Indian tribes oral tradition (Inbar and Risso, 2001a,b).

3. Samples and methods

3.1. Sampling strategy

Thirty-two hand-size rock samples were collected from fresh lava flows and scoria cones from the three volcanic systems (Los Volcanes, Payun Volcano and Payun Matru Volcano). Twelve basalts from the Los Volcanes field have been sampled over a surface covering the entire field (88Q, 88R, 88S, 88Y, 88AB, 94N, 94P, 94Q, 94W, 94U, 94V, 94AD and 94AF, Fig. 2). We sampled eight lava flows from the base to the summit of the Payun stratocone (94AR, 94AP, 88AC, 94AS, 94AN, 94AO, 94AQ and 94AT), together with a scoria cone at the base of the volcano (88AD). We have sampled lavas from the inner wall of the Payun Matru caldera (pre-collapse volcanism, samples 94AM and 94AH, Fig. 2) and from the ignimbrite (94T1, 94T2, and 88AA). Post-collapse lava flows filling the depression (94AI and 94AL, Fig. 2), lying on the external slopes (88Z and 94AE) and from a pumice fall deposit (94AG) were also sampled within the Payun Matru volcano.

3.2. Geochronology

We have used the K–Ar dating method based on the Cassignol–Gillot technique (Cassignol and Gillot, 1982; Gillot and Cornette, 1986) on carefully selected samples. In order to remove any possible gain of argon (excess argon) due to fluids circulations or from xenoliths of older basement rocks, and/or loss of potassium due to weathering, a careful mineralogical separation on the freshest samples was performed following thin sections examinations. Based on phenocrysts size, crushing and sieving at typically 125–250 μm and 250–500 μm were performed. Grains were ultrasonically washed with deionized water and a 10% nitric acid solution. Heavy liquids were used to keep groundmass or K-feldspars in narrow density ranges, and to remove mafic phenocrysts and, if present, any slightly weathered fraction. The density ranges are about 2.95–3.00 for basalts, 2.80–2.85 for intermediate rocks, and 2.60–2.65 for evolved lavas. Finally, a Frantz magnetic separator was used to further improve purity of the fraction. As K is preferentially concentrated in the last liquid phase, we have performed our analyses on groundmass separates, except for the pumice 94AG and lava flows 94AE and 94AL for which feldspars have been selected. Note that for these two samples, we have dated two size fractions (125–250 and 250–500 μm) at the same density range of 2.60–2.63 for sample 94AE, and two fractions of same size (125–250 μm) but different density ranges (2.51–2.60 and 2.60–2.61) for 94AL. Feldspars from the pumice 94AG were separated within the size range of 125–250 μm, and with a density between 2.56 and 2.62.

Potassium and argon were measured at the Laboratoire de Géochronologie Multi-techniques, Orsay (France), from different aliquots of the same mineral preparation, K by flame emission spectroscopy and Ar by mass spectrometry using an instrument similar to the one described in Gillot and Cornette (1986). The limit of detectability of the radiogenic Ar content is presently of 0.1% (Quidelleur et al., 2001) and makes the Cassignol–Gillot technique especially suitable for very young dating as it allows to obtain K–Ar ages as young as 2 ka with only a few centuries uncertainty (Gillot and Cornette, 1986). Such performance can be achieved because of the very stable analytic conditions of our mass spectrometer, which allows a very accurate atmospheric correction by direct comparison of the dated sample with an air aliquot measured in the exact same Ar pressure conditions. The relative uncertainty on K measurement is about 1% over a range of K contents between 0.1% and 15%. The calibration of the system is obtained by systematic measurements of an air pipette, which is routinely compared to the GL-O standard with its

Please cite this article in press as: Germa, A., et al. Volcanic evolution of the back-arc Pleistocene Payun Matru volcanic field (Argentina). J. S. Am. Earth Sci. (2010), doi:10.1016/j.jsames.2010.01.002

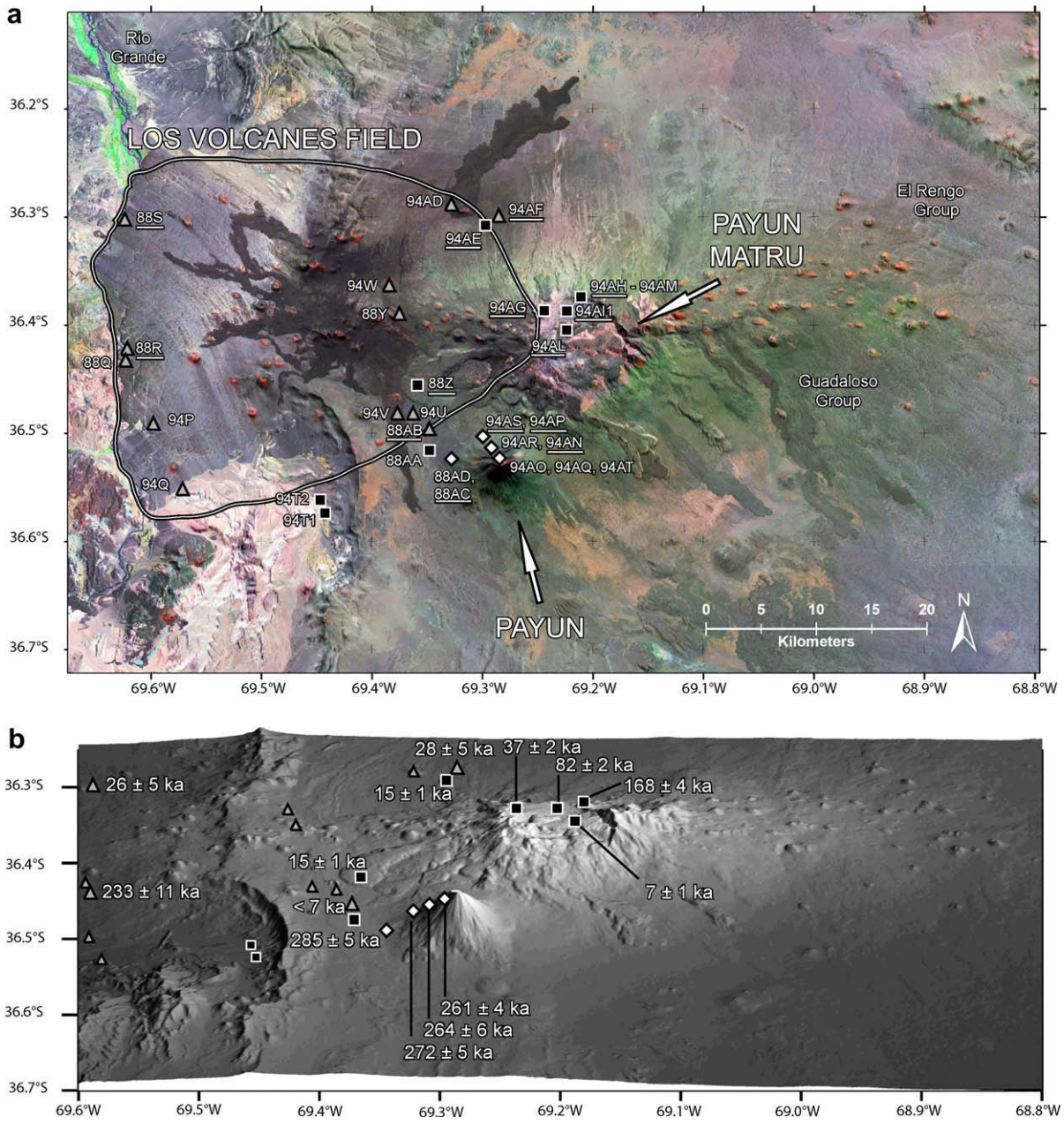

Fig. 2. (a) The Payun Matru volcanic field on the LANDSAT 7 satellite image: location of the 30 formations investigated. Grey triangles show the location of samples from Los Volcanes field, black squares are for Payun Matru samples, and white diamond for Payun samples. Underlined names indicate samples dated here and (b) digital elevation model at a resolution of 1:90,000 (DEM and SRTM data) of the studied area showing the K–Ar ages obtained in this study.

recommended value of 6.679×10^{-13} at. g^{-1} of radiogenic ^{40}Ar (Odin et al., 1982). Such calibration introduces an additional relative uncertainty of 1%, which leads to a total relative age uncertainty of about 1.5% for samples of about 1 Ma. However, for younger samples, the uncertainty due to the atmospheric correction dominates and can amount to 100% for sub-historic samples. Potassium and argon were analyzed at least twice in order to obtain a reproducible age within the range of error determined from periodic replicated measurements of dating standards, such as ISH-G, MDO-G (Gillot et al., 1992) and GL-O (Odin et al., 1982). For age calculations, decay constant and K isotopic ratios of Steiger and Jäger (1977) have been used. All uncertainties quoted here are given at the 1-sigma level. Analytical results are reported in Table 1.

3.3. Geochemistry

The whole-rock elementary compositions (major and trace elements) of the samples have been analyzed by Service d'Analyse des Roches et Minéraux (SARM) at Centre de Recherches Pétrographiques et Géochimiques, Nancy, France (CRPG). 200 mg of each sample were melted with $LiBO_2$ in Pt–Au crucible, and then dissolved with HNO_3. The solution obtained has been analyzed by ICP-AES (Thermo Electron IRIS Advantage) for major and minor elements, and/or by ICP-MS (Thermo Elemental X7) for 43 trace elements. Calibration has been made with international standards (AN-G, BR, UB-N, DR-N, GH), which underwent the same processing (Carignan et al., 2001; Govindaraju and Mevelle, 1987; Govindaraju et al., 1994). Results are provided in Table 2.

Please cite this article in press as: Germa, A., et al. Volcanic evolution of the back-arc Pleistocene Payun Matru volcanic field (Argentina). J. S. Am. Earth Sci. (2010), doi:10.1016/j.jsames.2010.01.002

Table 1
K–Ar ages obtained from groundmass and K-feldspar. Column heading indicate sample name, dated material (groundmass: G; K-feldspar: F), latitude, longitude, potassium content in percent, concentration of radiogenic ^{40}Ar in percent, number of atoms/g of radiogenic ^{40}Ar, age and 1-sigma uncertainty in ka, and average age and 1-sigma uncertainty in ka.

Sample	Material	Latitude, S	Longitude, W	K (%)	$^{40}Ar^*$ (%)	$^{40}Ar^*$ (at/g)	Age ± Un (ka)	Mean age (ka)
88AC	G	36°30′47.9″	69°20′43.5″	2.586	12.3	7.840E+11	290 ± 5	
					13.0	7.550E+11	280 ± 4	**285 ± 5**
94AP	G	36°29′42.6″	69°17′41.3″	3.800	9.7	1.084E+12	273 ± 5	
					7.8	1.070E+12	270 ± 5	**272 ± 5**
94AN	G	36°30′20.5″	69°17′27.6″	3.419	5.4	9.511E+11	266 ± 6	
					4.9	9.351E+11	262 ± 6	**264 ± 6**
94AS	G	36°29′16.9″	69°18′20.7″	3.601	19.8	9.907E+11	263 ± 4	
					20.8	9.756E+11	259 ± 4	**261 ± 4**
88R	G	36°25′26.0″	69°39′36.3″	1.299	2.2	3.023E+11	223 ± 11	
					2.4	3.274E+11	241 ± 11	**233 ± 11**
94AH1	G	36°22′26.1″	69°12′48.5″	4.757	5.5	8.404E+11	169 ± 4	
					6.7	8.332E+11	168 ± 3	**168 ± 4**
94AI1	G	36°22′49.1″	69°12′36.5″	3.792	7.2	3.256E+11	82 ± 2	
					10.1	3.267E+11	82 ± 1	**82 ± 2**
94AG	F	36°23′7.8″	69°14′6.9″	5.610	2.6	2.112E+11	36 ± 1	
					2.4	2.230E+11	38 ± 2	**37 ± 2**
94AF	G	36°18′28.6″	69°17′48.1″	0.874	0.6	2.740E+10	30 ± 5	
					0.6	2.434E+10	27 ± 5	**28 ± 5**
88Z	G	36°26′31.6″	69°22′50.6″	4.993	1.5	1.405E+11	27 ± 2	
					1.7	1.302E+11	25 ± 2	**26 ± 2**
88S	G	36°18′47.9″	69°39′50.3″	0.941	0.4	2.158E+10	22 ± 6	
					0.7	2.721E+10	28 ± 4	**26 ± 5**
94AE	$F_{250-500\ \mu m}$	36°18′34.3″	69°17′55.5″	5.514	1.6	8.382E+10	15 ± 1	
	$F_{125-250\ \mu m}$			5.503	1.1	9.442E+10	16 ± 2	**15 ± 1**
94AL	$F_{2.60-2.61}$	36°23′37.5″	69°13′08.8″	4.839	0.6	3.735E+10	7 ± 1	
	$F_{2.51-2.60}$			4.911	0.6	3.631E+10	7 ± 1	**7 ± 1**
88AB	G	36°28′55.8″	69°22′21.7″	1.028	<0.1	−8.402E+09	−8 ± 6	
					0.1	1.024E+10	10 ± 7	
					<0.1	−3.417E+08	0 ± 5	**<7**

3.4. Volume estimation

Volume estimates were determined using the GIS software ArcView 9.1, from analysis of the DEM (1:90,000) which utilizes a Universal Transverse Mercator (UTM) projection (19S zone) and the World Geodetic System 84 (WGS 1984) model. In order to evaluate the volumes of volcanic edifices, a three-dimensional surface was created. For the Payun volcano, which has a conical shape, we used the present shape and a simple calculation was made to refill the valleys. On the contrary, the summit of Payun Matru volcano has collapsed during the caldera-forming eruption, highlighting the need to model entire shield before this eruption. Eight radial profiles of the present shape of Payun Matru volcano have been drawn (Fig. 3a) and Bézier curves using the preserved slopes have been extrapolated to approximate a pre-collapse conic shape and to obtain a complete edifice with its summit (Fig. 3b). The selected profiles have been used to predict values at unsampled location and to interpolate a surface. The main technique used is a local polynomial interpolation (LPI) from ArcView 9.1 software, which creates a surface accounting for local variations only. The basal level has been estimated using the average elevation at the base of the outline of the Payun Matru volcano, and the underlying slope is extrapolated from the mean slope. The unit volume is then estimated by multiplying the basal area by the difference between the average elevation of the modeled edifice and those of the base level.

4. Results

4.1. Geochronology

Within 1-sigma uncertainty, all 14 K–Ar ages obtained here (Table 1) have been duplicated, which attests for the homogeneity of the mineralogical fraction selected. The mean age and uncertainty have been calculated by weighting each analysis with the amount of $^{40}Ar^*$ (Table 1). The ages range from 285 ± 5 ka to less than 7 ka. For the youngest ages (<50 ka), uncertainty is mainly a function of the radiogenic argon, and varies from 6 ka for basalts (88AB, 88S) to only 1 ka for trachytes (94AE, 94AL). Ages are also reported in Fig. 2b.

4.1.1. Payun volcano

The four K–Ar ages ranging between 285 ± 5 ka and 261 ± 4 ka (Table 1), demonstrate that the Payun volcano was built during Pleistocene. The oldest lava flow dated here (88AB, Fig. 2) is slightly away from the main cone and shows that Payun volcano probably started its construction around 285 ka. The three ages obtained on the main edifice (272 ± 5 ka, 264 ± 6 ka and 261 ± 4 ka) suggest that the volcano has been built within 2–20 kyr, and yield a mean age of 265 ± 5 ka.

4.1.2. Los Volcanes

The basaltic eruptions from the Payun Matru volcanic field preferentially occurred along the E–W direction, as evidenced by the distribution of strombolian cones, but are present all around the Payun Matru volcano. Because field access was limited, we only consider here the wide basaltic field Los Volcanes, located west of Payun Matru Volcano (Fig. 2). Two ages have been obtained for this area (Table 1). The thick prismatic lava flow, eroded into table-like aspect by the Rio Grande river (88R), has been dated at 233 ± 11 ka. Younger lava flow (such as 88S; 26 ± 5 ka), in some places, have filled the Rio Grande valley forming a natural damp, which was later eroded by the river into deep narrow canyons.

4.1.3. Payun Matru volcano

The oldest lava flow dated (sample 94AH1; 168 ± 3 ka) belongs to the NE inner topographic wall of the caldera and thus predates the caldera-forming eruption. This event has been associated with

Please cite this article in press as: Germa, A., et al. Volcanic evolution of the back-arc Pleistocene Payun Matru volcanic field (Argentina). J. S. Am. Earth Sci. (2010), doi:10.1016/j.jsames.2010.01.002

Table 2
Major element (wt.%) and trace element (ppm) of Payun Matru volcanic field.

	Los Volcanes												
	88Q	88R	88S	88Y	88AB	94Q	94P	94N	94AD	94AF	94U	94V	94W
wt.%													
SiO_2	48.75	46.98	47.66	47.84	46.97	49.10	48.71	46.51	48.88	48.8	47.28	46.66	48.60
TiO_2	1.63	2.46	1.80	2.09	1.89	2.32	1.76	1.96	1.79	2.11	1.85	2.15	1.84
Al_2O_3	16.91	17.49	17.36	18.72	17.68	16.64	16.10	16.55	17.15	16.51	17.56	17.35	16.67
Fe_2O_3	10.31	12.13	10.95	11.28	11.38	11.74	11.23	11.46	11.00	11.76	11.14	11.63	10.68
MnO	0.15	0.18	0.15	0.16	0.16	0.17	0.17	0.17	0.16	0.16	0.17	0.17	0.16
MgO	6.71	4.76	7.42	5.52	6.43	5.64	7.96	6.82	6.39	6.87	5.75	6.77	6.90
CaO	9.53	8.69	10.31	8.51	10.49	8.66	9.64	10.12	9.28	10.59	10.43	11.06	10.30
Na_2O	3.22	3.86	3.59	4.34	3.47	4.23	3.59	3.52	3.85	3.38	3.71	3.51	3.47
K_2O	1.56	1.47	1.04	1.53	1.13	1.531	1.39	1.16	1.21	1.02	1.021	1.15	1.24
P_2O_5	0.35	0.73	0.33	0.61	0.39	0.65	0.40	0.43	0.48	0.38	0.50	0.42	0.43
LOI	0.81	0.41	−0.73	−0.69	−0.10	−0.01	0.02	0.33	0.06	0.40	0.76	−0.20	0.36
Total	99.93	99.16	99.88	99.91	99.89	100.65	100.96	99.02	100.44	100.06	100.35	100.66	100.64
ppm													
Rb	27.7	19.5	14.4	26.2	19.4	25.8	30.7	20.7	32.4	13.8	23.8	20.3	25.6
Ba	348	430	269	475	296	332	300	286	323	234	358	287	336
Th	5.10	2.42	1.28	2.88	2.21	3.40	4.02	2.55	3.94	1.50	2.92	1.76	2.84
U	1.23	0.67	0.41	0.85	0.67	0.86	1.20	0.74	1.09	0.45	0.85	0.57	0.80
Nb	20.5	27.1	13.7	23.3	14.6	23.2	17.7	15.9	18.9	13.9	17.3	16.3	16.7
Ta	1.54	1.87	0.96	1.60	1.08	1.78	1.37	1.19	1.45	1.04	1.27	1.25	1.24
La	22.0	30.3	15.5	28.1	18.7	23.1	19.7	18.3	21.5	14.0	21.5	17.0	19.7
Ce	45.7	63.6	34.6	59.3	40.5	49.7	42.0	39.2	44.6	31.1	47.0	38.8	43.2
Pb	5.20	2.96	2.49	3.92	5.63	3.51	4.23	2.97	4.45	2.11	3.88	2.40	3.60
Pr	5.72	8.21	4.70	7.65	5.45	6.49	5.38	5.185	56.495	4.20	6.14	5.18	5.59
Sr	870	905	560	918	624	628	556	623	604	553	723	668	618
Nd	24.1	34.9	20.6	32.2	23.8	27.7	22.7	22.1	23.5	18.6	25.8	22.9	23.8
Zr	190	178	159	217	154	186	174	147	188	133	176	153	173
Hf	4.57	4.09	3.66	4.81	3.63	4.46	4.11	3.48	4.35	3.23	4.07	3.64	4.00
Sm	5.41	7.58	4.95	7.02	5.55	6.39	5.18	5.24	5.45	4.79	5.86	5.45	5.50
Eu	1.74	2.57	1.76	2.36	1.87	2.19	1.74	1.84	1.78	1.71	2.00	1.93	1.86
Gd	4.95	6.67	4.72	6.19	5.24	6.12	4.99	5.08	5.13	4.72	5.46	5.22	5.26
Tb	0.76	0.99	0.73	0.90	0.79	0.91	0.74	0.75	0.7	0.72	0.80	0.79	0.76
Dy	4.31	5.34	4.16	4.92	4.44	5.10	4.28	4.30	4.41	4.27	4.56	4.53	4.44
Y	23.3	27.8	22.2	26.0	23.5	25.7	21.9	21.8	23.0	21.3	23.8	22.8	23.0
Ho	0.83	0.98	0.80	0.91	0.83	0.95	0.780	0.79	0.82	0.8	0.84	0.84	0.82
Er	2.25	2.57	2.15	2.47	2.24	2.55	2.20	2.14	2.23	2.07	2.29	2.23	2.18
Tm	0.32	0.35	0.31	0.35	0.32	0.36	0.32	0.350	0.31	0.28	0.32	0.31	0.31
Yb	2.13	2.20	1.95	2.20	2.061	2.30	2.03	1.92	2.06	1.82	2.07	1.95	1.99
Lu	0.32	0.32	0.29	0.33	0.31	0.34	0.30	0.28	0.31	0.27	0.30	0.29	0.29

	Payun								
	88AC	88AD	94AN	94A0	94AP	94AQ	94AR	94AS	94AT
wt.%									
SiO_2	63.46	51.61	53.86	53.82	62.61	58.86	62.84	62.28	55.96
TiO_2	0.74	2.21	1.90	1.92	0.91	1.37	0.84	0.90	1.63
Al_2O_3	17.39	18.13	16.74	16.74	17.19	16.92	17.00	17.21	16.77
Fe_2O_3	4.52	9.63	9.57	9.62	5.28	7.05	5.12	5.20	8.13
MnO	0.14	0.17	0.18	0.18	0.15	0.14	0.15	0.15	0.16
MgO	0.56	2.93	2.80	2.79	1.09	1.99	0.95	1.06	2.33
CaO	1.83	6.49	5.60	5.44	2.41	4.25	2.17	2.39	5.15
Na_2O	5.79	4.95	5.04	5.05	5.98	5.05	6.00	5.97	5.04
K_2O	4.60	2.67	3.24	3.22	4.19	3.76	4.37	4.20	3.43
P_2O_5	0.23	0.75	0.95	0.97	0.35	0.62	0.31	0.35	0.82
L.O.I.	0.66	−0.04	0.31	0.28	0.06	0.05	0.25	0.16	0.63
Total	99.92	99.50	100.18	100.03	100.22	100.05	99.99	99.86	100.06
ppm									
Rb	100	53.8	71.6	70.6	86.6	92.3	91.6	87.6	78.2
Ba	783	527	556	551	907	644	898	901	576
Th	11.8	6.32	8.93	9.12	9.96	12.0	10.4	9.98	10.9
U	3.03	1.82	1.60	1.96	1.24	2.58	1.86	1.16	2.53
Nb	46.6	38.8	48.2	48.1	47.6	44.8	49.0	48.2	47.2
Ta	3.67	2.92	3.59	3.53	3.34	3.54	3.49	3.30	3.81
La	52.3	40.4	46.8	46.4	51.0	44.5	49.8	49.6	45.5
Ce	96.0	83.5	94.1	95.1	96.9	87.4	96.5	96.1	91.6
Pb	28.8	6.03	7.49	7.85	8.90	9.41	10.1	16.3	7.79
Pr	10.5	10.4	11.4	11.5	10.9	9.94	10.8	10.8	10.5
Sr	264	797	581	568	336	536	277	331	533
Nd	37.5	42.3	44.6	45.9	40.9	37.7	39.4	40.1	41.1
Zr	493	319	380	378	436	392	457	442	364
Hf	9.71	6.52	7.83	8.05	8.83	7.90	9.34	8.64	7.76
Sm	6.84	8.90	9.09	9.21	7.72	7.37	7.45	7.68	8.27
Eu	1.68	2.65	2.50	2.52	2.28	1.94	2.08	2.17	2.20

Please cite this article in press as: Germa, A., et al. Volcanic evolution of the back-arc Pleistocene Payun Matru volcanic field (Argentina). J. S. Am. Earth Sci. (2010), doi:10.1016/j.jsames.2010.01.002

Table 2 (*continued*)

	Payun								
	88AC	88AD	94AN	94A0	94AP	94AQ	94AR	94AS	94AT
Gd	5.74	7.84	8.15	8.08	6.59	6.30	6.25	6.26	7.08
Tb	0.88	1.15	1.18	1.19	0.99	0.95	0.98	0.97	1.06
Dy	5.10	6.29	6.75	6.74	5.81	5.32	5.65	5.56	5.98
Y	29.4	33.1	34.6	34.0	32.0	28.5	31.6	31.6	31.9
Ho	0.98	1.15	1.22	1.23	1.1	1.00	1.08	1.07	1.12
Er	2.86	3.12	3.29	3.33	3.21	2.75	3.06	3.02	3.11
Tm	0.46	0.45	0.48	0.50	0.49	0.42	0.46	0.47	0.46
Yb	3.08	2.92	3.17	3.25	3.25	2.80	3.24	3.23	3.09
Lu	0.50	0.45	0.50	0.50	0.51	0.44	0.51	0.50	0.47
	Payun Matru								
	94T1	94T2	94AH1	94 AI1	94AL	94AE	94AG	88Z	88AA
wt.%									
SiO_2	62.55	60.94	63.26	58.99	67.16	67.01	65.17	68.80	63.26
TiO_2	0.74	0.73	0.73	1.28	0.48	0.43	0.39	0.39	0.67
Al_2O_3	17.61	17.05	17.49	17.68	16.22	15.85	14.71	16.07	18.34
Fe_2O_3	4.21	4.19	4.41	6.05	3.19	3.11	3.08	3.07	3.73
MnO	0.11	0.11	0.12	0.15	0.12	0.12	0.12	0.12	0.09
MgO	1.05	1.10	1.06	1.56	0.38	0.35	0.38	<L.D.	0.74
CaO	3.36	3.74	2.66	3.49	0.84	0.83	0.81	0.49	2.18
Na_2O	5.38	5.04	5.45	5.65	5.97	5.62	5.03	5.72	5.83
K_2O	4.58	4.37	4.53	4.16	5.54	5.60	5.15	5.28	4.66
P_2O_5	0.26	0.20	0.27	0.46	0.09	0.09	0.09	0.09	0.27
L.O.I.	0.89	2.75	0.23	0.19	0.32	1.18	4.74	0.13	0.14
Total	100.73	100.22	100.19	99.66	100.30	100.19	99.68	100.16	99.91
ppm									
Rb	143	134	142	91.0	208	236	259	253	150
Ba	603	588	527	688	185	76.9	33.3	99.6	604
Th	20.1	18.9	21.0	16.1	31.2	34.3	45.1	39.5	21.8
U	5.92	5.31	6.02	3.05	8.91	9.68	12.4	9.70	5.99
Nb	49.2	46.9	53.0	53.8	83.3	89.2	108	101	53.9
Ta	4.18	4.03	4.55	4.10	7.02	7.57	8.88	8.56	4.59
La	37.5	35.3	36.7	43.7	59.5	58.6	65.1	68.5	39.4
Ce	72.5	68.5	71.1	90.4	112	113	129	131	74.7
Pb	12.4	14.2	11.6	14.0	13.2	18.2	24.3	12.1	20.9
Pr	7.86	7.35	7.81	10.5	12.1	12.2	13.3	13.8	8.34
Sr	316	322	344	392	33.4	23.3	12.6	30.7	310
Nd	27.4	26.1	27.3	39.3	41.3	39.5	43.9	45.2	29.8
Zr	528	500	577	549	990	896	757	893	595
Hf	11.2	10.6	11.9	11.1	20.9	19.3	19.7	19.8	12.2
Sm	5.25	4.95	5.22	8.06	7.42	7.31	8.24	8.16	5.68
Eu	1.34	1.35	1.30	2.22	0.73	0.42	0.29	0.47	1.42
Gd	4.52	4.20	4.40	6.86	6.17	5.84	6.46	6.63	4.71
Tb	0.72	0.69	0.71	1.08	1.07	1.05	1.15	1.15	0.78
Dy	4.26	4.00	4.12	6.23	6.85	6.48	7.27	6.99	4.55
Y	24.9	23.8	24.2	31.6	40.7	41.3	44.8	44.6	26.8
Ho	0.83	0.79	0.82	1.14	1.38	1.33	1.47	1.43	0.89
Er	2.46	2.32	2.50	3.32	4.25	4.20	4.65	4.55	2.68
Tm	0.40	0.39	0.41	0.49	0.74	0.780	0.80	0.78	0.44
Yb	2.92	2.79	2.95	3.46	5.20	5.27	5.89	5.63	3.13
Lu	0.47	0.45	0.47	0.55	0.86	0.87	0.96	0.91	0.51

the El Portezuelo large extend ignimbritic phase. Unfortunately, dating of both 94T2 and 88AA from this formation was not conclusive because of weathering of the dominant glass fraction, the lack of juvenile minerals, and the occurrence of inherited material from basement rocks due to the explosivity of the eruption. Sample 94AI1, from an intra-caldera trachyandesite flow from the El Mollar group (Gonzales Diaz, 1970), has been dated at 82 ± 1 ka. A white pumice fall deposit (La Planchada (Gonzales Diaz, 1972)), dated at 37 ± 1 ka (94AG), covers the external and internal slopes of the northwestern rim. The youngest activity within the caldera (Gonzales Diaz, 1970), the Escorial del Matru, has been dated at 7 ± 1 ka (94AG, Table 1). On the NW external slope of the volcano, about four lava flows were emitted from a SW-NE fissure. The longest has been dated at 15 ± 1 ka (94AE) and overlies an older basaltic flow (94AF) dated at 28 ± 5 ka. On the western flank, a massive rhyolitic lava flow (88Z) from the La Calle group (Gonzales Diaz, 1972) has been dated at 26 ± 1 ka. To the south of this flow, the ignimbrite deposit is partially covered by a trachyandesitic lava flow, which yielded a recent age of less than 7 ka (88AB, Table 1).

4.2. Petrography and geochemistry

4.2.1. Petrography

Basalts from the Los Volcanes field have been sampled over a surface covering the entire field. Most of them have a fluidal microlitic texture and contain numerous phenocrysts of olivine (sizes from 0.2 to 2 mm). Many opaque minerals are also observed. These rocks are fine to medium grained, with 2–10% phenocrysts. Regarding the Payun Matru volcano, we have sampled lavas from the pre-collapse volcanism (Group 1: 94AM and 94AH from the caldera walls, and 94T1, 94T2 and 88AA from the ignimbrite deposit) and from the post-collapse volcanic activity (Group 2) from lava flows filling the depression (94AI and 94AL), lying on the external slopes (88Z, 94AE) and from a pumice fall deposit (94AG). The groundmass of rocks from Group 1 is glassy and

Please cite this article in press as: Germa, A., et al. Volcanic evolution of the back-arc Pleistocene Payun Matru volcanic field (Argentina). J. S. Am. Earth Sci. (2010), doi:10.1016/j.jsames.2010.01.002

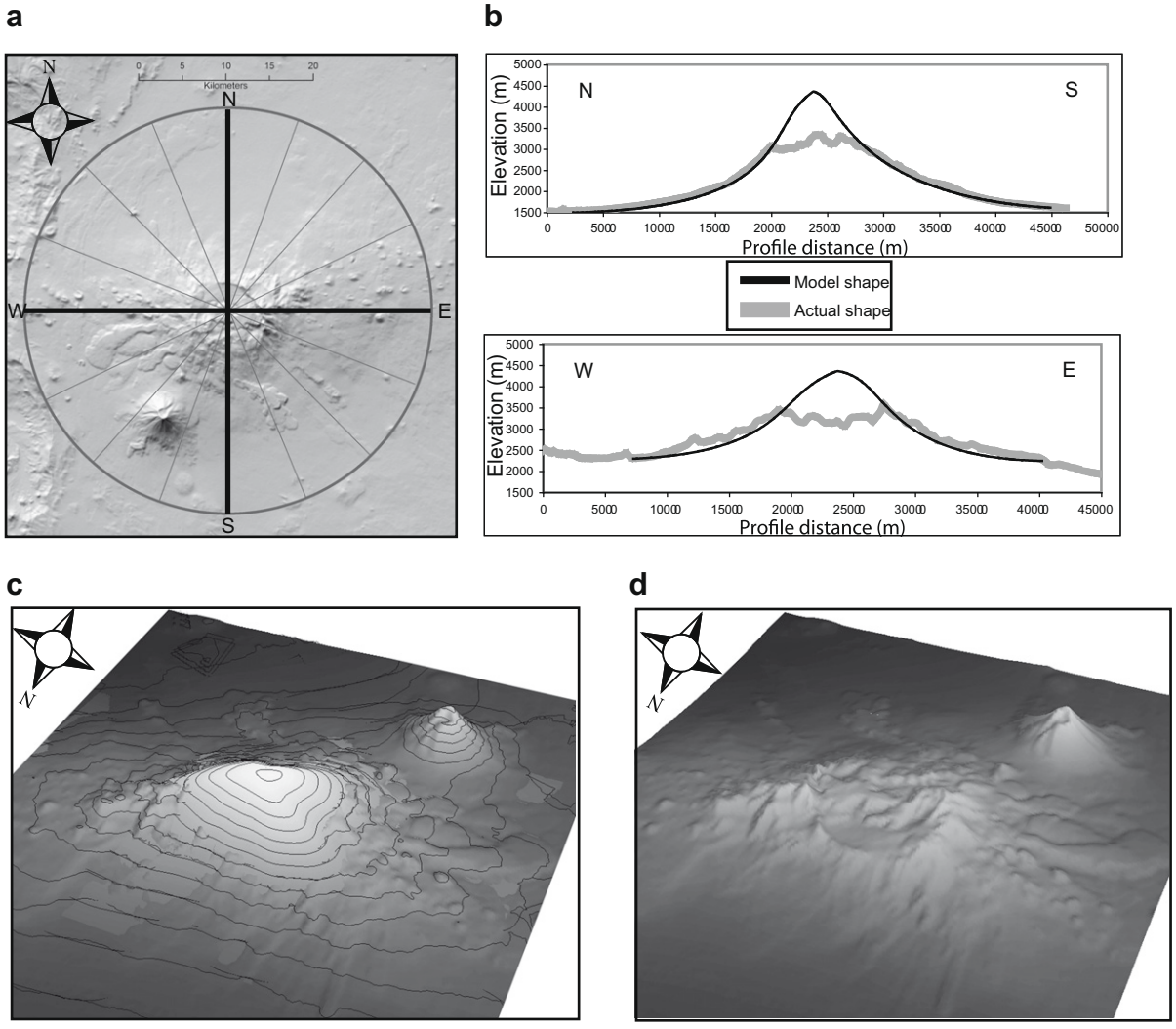

Fig. 3. (a) Location of the eight radial profiles centered on the Payun Matru volcano, used in b. (b) N–S and E–W profiles of extrapolated topography (black lines), which is based on the present day external slopes (grey lines). (c) Modeled DEM and elevation curves for the Payun Matru volcano before the caldera-forming eruption and (d) for sake of comparison, DEM of the present volcanic field.

encloses 25–30 vol.% of phenocrysts, mainly plagioclase with some sanidine and small clinopyroxene. The Group 2 displays a more microlitic groundmass, with intersertal glass, but with more phenocrysts (30–40 vol.%). Fresh sanidine is the predominant mineral and no plagioclase can be found, except in sample 94AE where a cluster of coarse plagioclases can be observed. Although sample 94AI belongs to the Group 2, it still has more plagioclase than sanidine and clinopyroxene. In addition, samples 88AA and 94AG, from explosive volcanism, are essentially constituted of volcanic glass and have a porous and fragmental texture comprising crystals of sanidine and clinopyroxene of 1–3 mm in size, embedded in a glassy and porous groundmass. All the trachytic lavas from Payun volcano can be separated into two groups. Thin sections from the Group 3 (94AN, 94AT, 94AO, 94AQ and 88AD) have small but numerous phenocrysts (20–25%). The groundmass is constituted for a large part of glass. Rocks from the Group 4 (94AR, 94AP, 94AS and 88AC) are medium to coarse grained, with 5–10% phenocrysts. In general, most phenocrysts are constituted of prismatic and large zoned plagioclase with size ranging from 1 to more than 2 mm, while others are sanidine and rare small clinopyroxene. Phenocrysts are enclosed within a microlitic groundmass constituted of plagioclase and intersertal glass.

4.2.2. Major elements

In the total alkali vs. silica (TAS) diagram (Fig. 4) (Le Bas et al., 1986), the analyzed volcanic rocks fall within the basalt, trachybasalt, basaltic-trachyandesite, trachyandesite and trachyte fields, but basalts fall close to the boundary with the sub-alkaline series. All lavas are more alkaline than volcanic rocks of the main arc and belong to calc-alkaline series in agreement with earlier studies (Bermudez et al., 1993). Silica contents range between 46.5 wt.% and 68.8 wt.% and alkali contents between 3.8 wt.% and 10.3 wt.%. In the K_2O vs. SiO_2 diagram (Fig. 5a), samples from Payun and Payun Matru lie in the shoshonitic series and high-K series domain, whereas samples from Los Volcanes field fall close to the calc-alkaline domain. Taking into account the very low loss on ignition (L.O.I.) of the rocks from Payun Matru volcanic field (except for 94T1, 94T2 and pumice 94G), we did not recalculate the data to an anhydrous basis. From basalts to rhyolites, there is a strong decrease of TiO_2 (2.6–0.5 wt.%), Fe_2O_3 (12.5–3.1 wt.%), MgO (8.5–0.1 wt.%) and CaO (11–0.5 wt.%). Al_2O_3 concentrations show a large variability in Los Volcanes basalts (16–19 wt.%) and increase from 16.5 to 18.5 wt.% (between 50 and 63 wt.% SiO_2), to decrease suddenly to 16 wt.% for the most evolved rocks of Payun Matru. The variation of P_2O_5 concentrations across the data set is marked by

Please cite this article in press as: Germa, A., et al. Volcanic evolution of the back-arc Pleistocene Payun Matru volcanic field (Argentina). J. S. Am. Earth Sci. (2010), doi:10.1016/j.jsames.2010.01.002

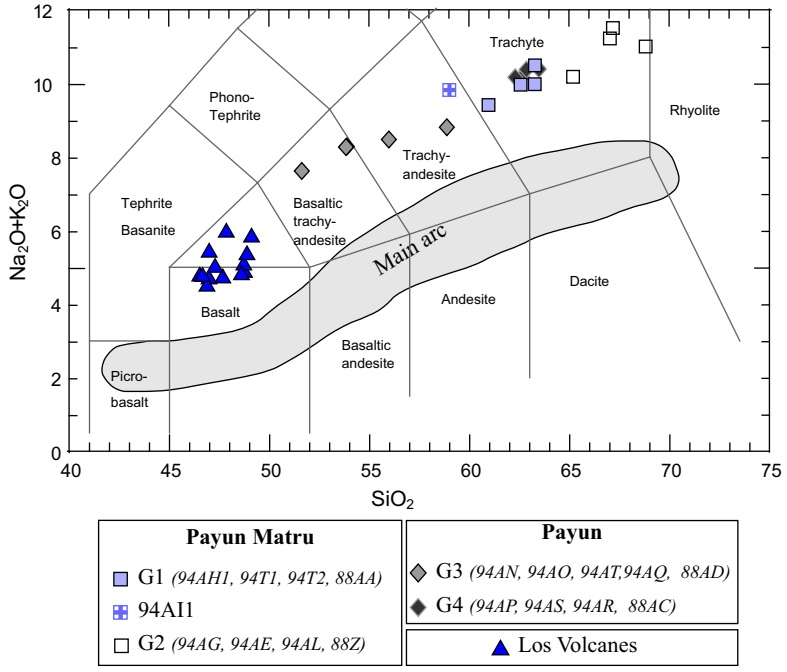

Fig. 4. $K_2O + Na_2O$ vs. SiO_2 classification diagram (Le Bas et al., 1986) for samples from the SVZ main arc (grey domain, data from GEOROC (Sarbas and Nohl, 2008), www.georoc.mpch-mainz.gwdg.de) and from the Payun Matru volcanic field (this study). Triangles are for Los Volcanes rocks, diamonds for Payun samples, and squares for Payun Matru rocks.

an increase in the basic rock interval (0.3–1% between 46.51 and 54 wt.% SiO_2) and a rapid decrease (1–0.1 wt.%) for the most evolved compositions (55–70 wt.% SiO_2).

4.2.3. Trace elements

Rare earth element (REE) patterns normalized to CI carbonaceous chondrites (Sun and McDonough, 1989) show an enrichment in LREE as illustrated in Fig. 6, with $(La/Yb)_N$ ratio ranging from 4.7 to 12.1. Samples from Los Volcanes display rather homogeneous patterns (Fig. 6a), with light LREE enrichment. Diagram for Payun volcano rocks (Fig. 6b) generally has a higher but rather similar enrichment in LREE, while strong differences are observed for Payun Matru volcano rocks (Fig. 6c). For the latter, we can distinguish three groups based on the shape of the REE patterns and the silica contents. First, 94AI1 (59 wt.% SiO_2), has a different and flat pattern compared to the other samples. It is a lava flow from the caldera floor, probably one of the first flows emitted after the collapse. Rocks from the inner wall of the caldera and from the ignimbrite constitute a distinct group (60–63 wt.% SiO_2) showing enrichment in HREE (G1: 94AH1, 94T1, 94T2, 88AA). Younger samples from lava flows located inside the depression and on the flanks of the volcano (G2: 94AG, 88Z, 94AE, 94AL; 65–68 wt.% SiO_2) have a light enrichment in LREE, and significant negative Eu anomalies.

In the spider diagram (Fig. 7a) normalized to primordial-mantle (Sun and McDonough, 1989), Los Volcanes rocks are characterized by enrichment of incompatible elements of low ionic potential (Rb, Ba and Sr) and low abundances of elements of high ionic potential (Nb, Ta, Zr, Hf, Ti and Y) like oceanic island basalts (OIB). For the Payun volcano (Fig. 7b), two groups are distinguished based on their silica contents ranging from 54 to 59 wt.% (G3: 94AN, 94AO, 94AQ, 94AT, 88AD) and between 62 and 63 wt.% (G4: 88AC, 94AP, 94AS and 94AR), respectively. Rocks from Payun Matru volcano (Fig. 7c) can be divided into the same Groups G1 and G2 as defined using the REE diagrams (Fig. 6). For both volcanoes, Fig. 7b and c display positive Th, U, Ta, Pb, Zr anomalies and negative Ba, Nb, Sr, Eu, Ti anomalies.

Fig. 8 shows a bivariate diagram with Ba/Ta as a function of La/Ta, which is of particular interest to discriminate between geodynamic settings for South America volcanic rocks: increasing Ba/Ta ratios indicate increasing fluids and crustal components, whereas increasing La/Ta ratios indicate increasing arc-like signatures (Kay, 2005; Kay and Mpodozis, 2002). Intraplate and back-arc calc-alkaline group samples have been defined with Ba/La ratios from 12 to 15, while CVZ frontal arc rocks have Ba/La ratios greater than 18. Samples from the Payun Matru volcanic field studied here show La/Ta ratios lower than 18, and Ba/La ratios between 11 and 20 (Fig. 8), and then fall within the intraplate to far back-arc domains as defined by Kay et al. (2005). Three samples display much lower Ba/La ratios, due to Ba depletion (Ba < 200 ppm, Table 2): 94AE, 94AL and 88Z, the youngest and most evolved samples (with SiO_2 greater than 65 wt.%, Fig. 4) within the Payun Matru caldera (Fig. 2).

5. Discussion

5.1. Temporal evolution: ages and morphology

The activity of the basaltic field of Los Volcanes has been dominated by effusive and strombolian activity since at least 300 ka, over at least 3000 km^2.

The Payun volcano has a volume estimated at 40 km^3. It has been built between 272 ± 5 and 261 ± 4 ka (Table 1), which yield a duration of about 11 kyr. A construction rate of about 4×10^{-3} km^3 yr^{-1} can be inferred, which is on the same order than the average output rate of $4.4 \pm 0.8 \times 10^{-3}$ km^3 yr^{-1} on continental crust (White et al., 2006), of some silicic volcanoes from continental arcs (Mt St Helens: 1.98×10^{-3} km^3 yr^{-1}; Volcan San Juan 1.78×10^{-3} km^3 yr^{-1}), or from continental volcanic field (Davis mountains, Texas 1.0×10^{-3} km^3 yr^{-1}). It is of the same order of magnitude than the minimum eruptive rate of ignimbrite volcanism of the Altiplano Puna volcanic complex (de Silva and Gosnold, 2007). Note that, however, the eruption rate of Payun volcano is an

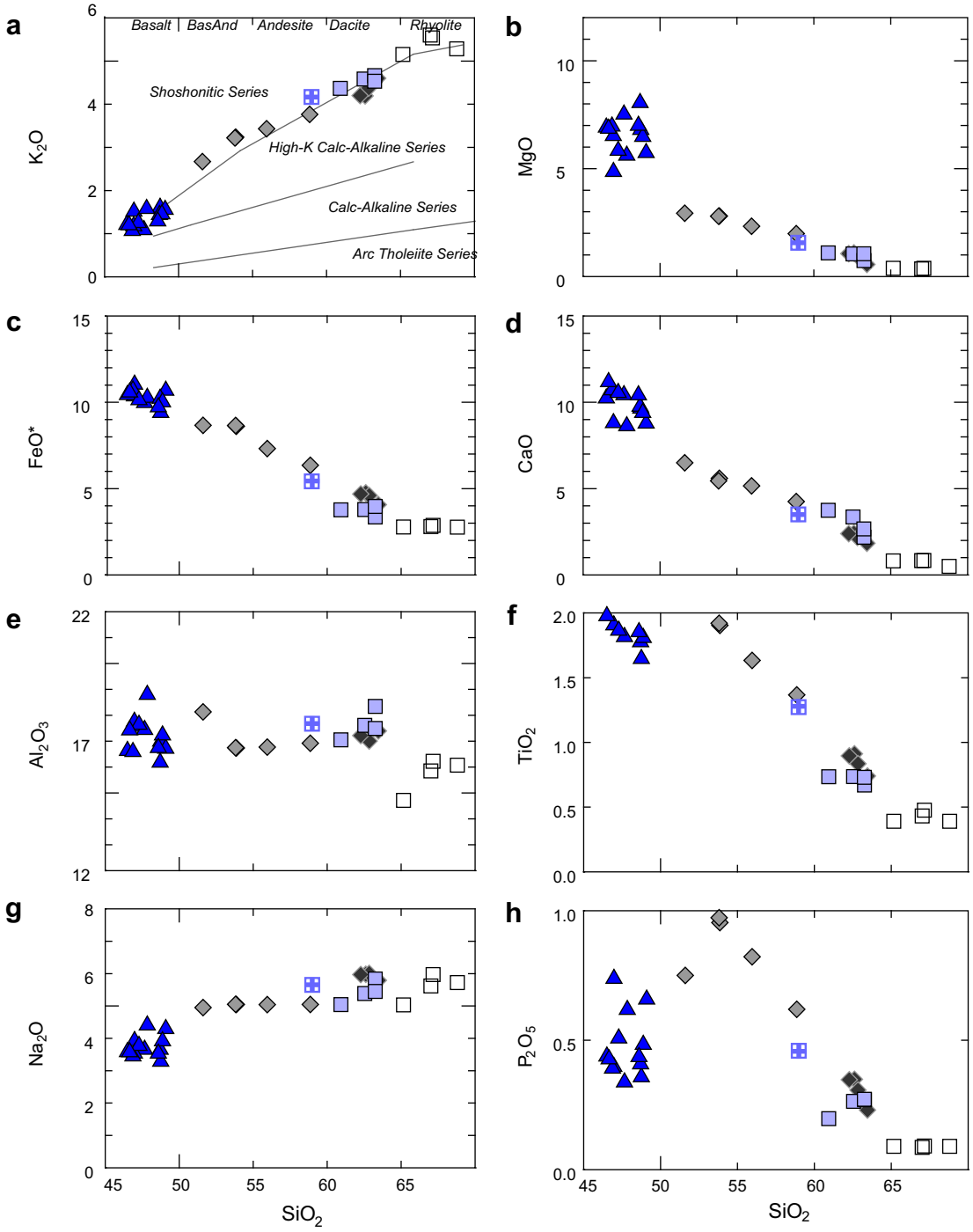

Fig. 5. (a) K_2O vs. SiO_2 classification diagram (Peccerillo and Taylor, 1976) for Payun Matru volcanic field volcanics (symbols as in Fig. 3). (b–h) Variation diagrams for MgO, FeO^*, CaO, Al_2O_3, TiO_2, Na_2O and P_2O_5 (wt.%) vs. SiO_2 (wt.%) for Payun Matru volcanic field volcanic (symbols as in Fig. 3).

order of magnitude higher than the peak eruption rates of 0.2–0.3 $\times 10^{-3}$ km^3 yr^{-1} calculated for two young volcanoes from the Tatara–San Pedro volcanic complex (Singer et al., 1997), located on the Andean range at the same latitude than Payun Matru volcanic field and constructed within 930 kyr. The growth rate of these complex based on preserved deposits has been estimated at 0.06 $\times 10^{-3}$ km^3 yr^{-1} (Singer et al., 1997). The back-arc extensional setting location could explain such difference. It is likely that the eruptive rate calculated for the Payun volcano is higher than volcanoes located at the same latitude within the Andean range because, there, compressional forces and thick rock pile could strongly limit magma ascent towards the surface.

Based on our new radiometric ages and geochemical analyses, we constrain the Payun Matru volcano activity in the last 300 kyr rather than during Pliocene, as previously inferred (Kay et al., 2006; Ramos and Kay, 2006). However, the still limited number of ages available (Table 1) prevents us to estimate the output rate for this volcano. The Payun Matru volcano has a complex morphology and younger lava flows and domes cover its western and eastern flanks, hiding its basal limit. We constrain between 168 ± 3 ka (inner caldera wall) and 82 ± 1 ka (lava flow inside the depression) the caldera-forming eruption. With a GIS reconstruction, the ancient volcano has been modeled as a flattened cone, about 2300 m high, with a basal diameter of about 20 km, and therefore

Please cite this article in press as: Germa, A., et al. Volcanic evolution of the back-arc Pleistocene Payun Matru volcanic field (Argentina). J. S. Am. Earth Sci. (2010), doi:10.1016/j.jsames.2010.01.002

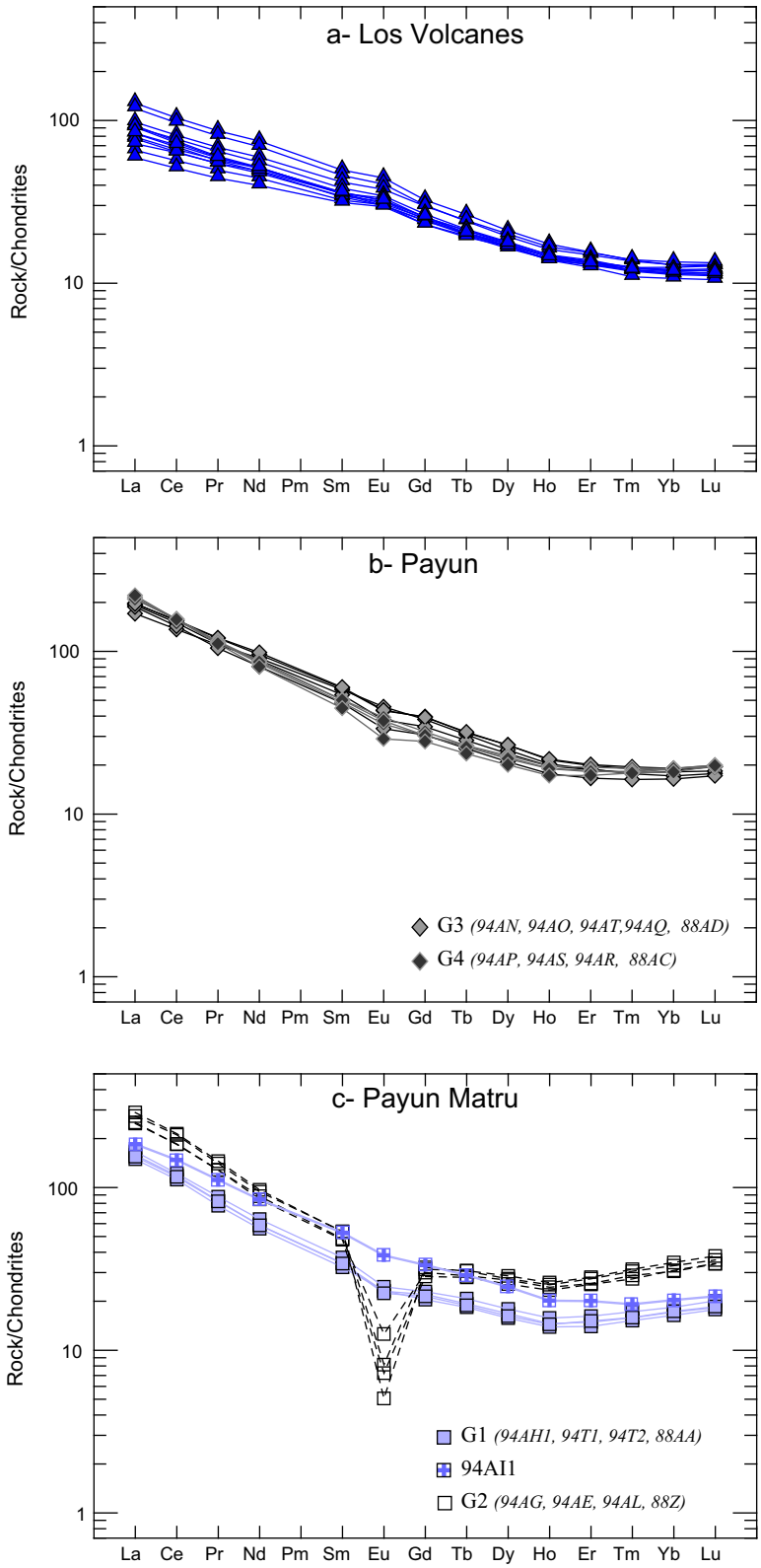

Fig. 6. Chondrite-normalized REE spectra for (a) Los Volcanes, (b) Payun and (c) Payun Matru rocks. Normalizing values of CI carbonaceous chondrites from Sun and McDonough (1989).

a volume of about 240 km^3 (Fig. 3c). Considering that the actual caldera floor is about 3000 m above sea-level, or 1000 m above the basement (younger lava flows excepted), we can roughly calculate that the volume removed by the caldera-forming eruption is about 25 km^3.

5.2. Magmatic evolution

Our results show that lavas from the Los Volcanes field were subjected to only a slight fractional crystallization of olivine and oxides (Fig. 5). As shown by their spatial distribution (Fig. 3a), they erupted

Please cite this article in press as: Germa, A., et al. Volcanic evolution of the back-arc Pleistocene Payun Matru volcanic field (Argentina). J. S. Am. Earth Sci. (2010), doi:10.1016/j.jsames.2010.01.002

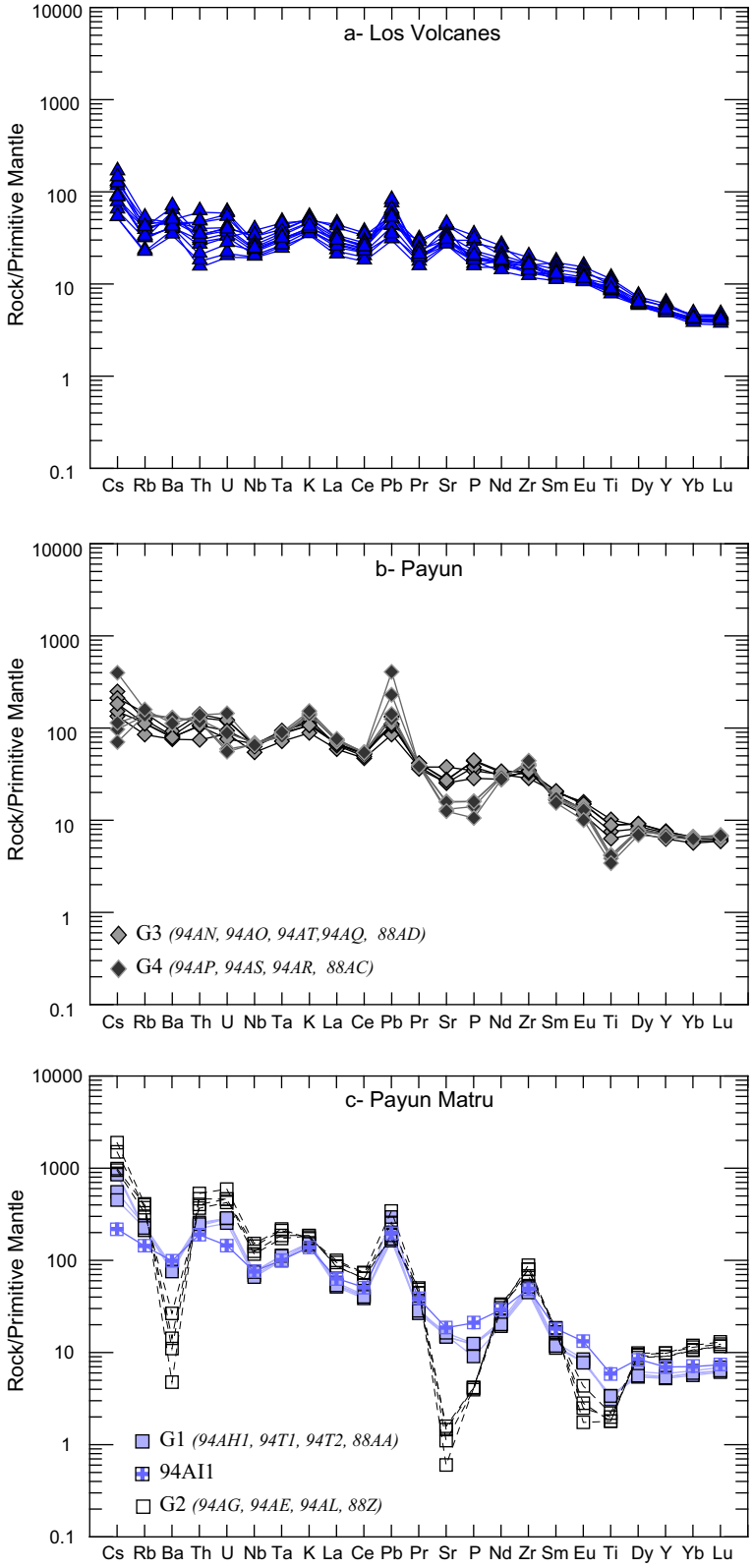

Fig. 7. Primitive mantle normalized trace element spectra for (a) Los Volcanes, (b) Payun and (c) Payun Matru rocks. Normalizing values from Sun and McDonough (1989).

along an overall WE preferential direction. Magma ascent from the reservoir to the surface through pre-existing EW faults was probably favored by crustal extension into a back-arc tectonic setting.

Payun and Payun Matru volcanoes seem to evolve by crystal fractionation of Cpx + Fe – Ti oxides + apatite + plagioclases from the same source (Fig. 5). It seems that apatite starts to crystallize in the reservoir before the magma ascent, as shown by the P_2O_5 variation. Plagioclase, sanidine, apatite and magnetite fractionation is also characterized by Ba, Eu, Sr and Ti negative anomalies in evolved rocks (Figs. 5 and 6). Evolved samples from Payun Matru

Please cite this article in press as: Germa, A., et al. Volcanic evolution of the back-arc Pleistocene Payun Matru volcanic field (Argentina). J. S. Am. Earth Sci. (2010), doi:10.1016/j.jsames.2010.01.002

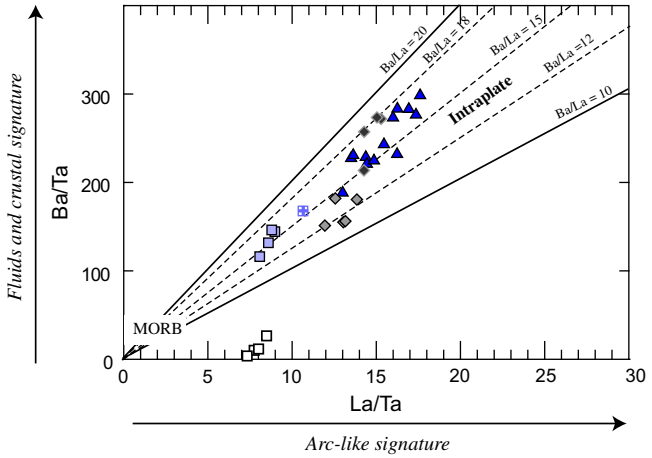

Fig. 8. Ba/Ta vs. La/Ta diagram for Payun Matru volcanic field rocks (symbols as in Fig. 3). Increasing Ba/Ta ratios indicate increasing fluids and crustal components, whereas increasing La/Ta ratios indicate increasing arc-like signatures.

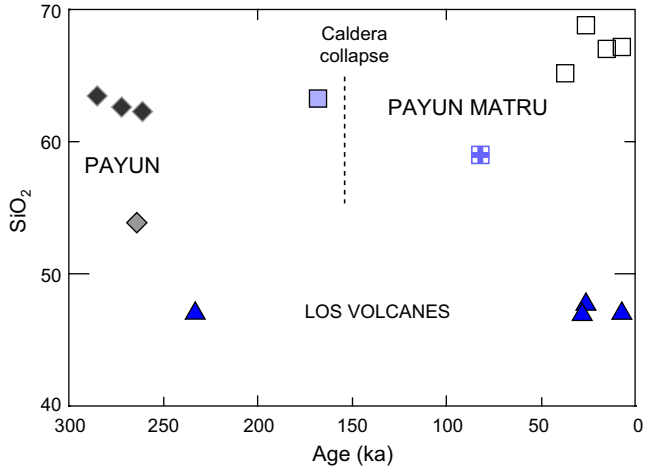

Fig. 9. SiO_2 vs. Age (in ka) diagram for samples from the Payun Matru volcanic field (symbols as in Fig. 3).

volcanoes also show positive Th and negative Nb anomalies, associated with Ba depletion (<200 ppm), which then cannot be interpreted as a source signature. Unfortunately, the lack of isotopic measurements makes difficult to better constrain the magmatic sources and subsequent evolution through time. Fig. 9 shows that the SiO_2 content of pre-collapse lava of the Payun Matru volcano (94AH1) is significantly higher than the oldest post-collapse flow (94AI). This can be explained by the partial destruction of the volcano and the subsequent release of edifice load, which may favor renewed eruption of more basic magmas (Pinel and Jaupart, 2000) after the collapse. The deloading first allowed basic magmas to erupt (94AI), followed by intermediate to highly differentiated lavas, inside and outside the caldera. As the shield grew, magmas ascent and eruption though the central vent complex was made more difficult (Davidson and de Silva, 2000), and the accumulation of lavas allowed storage and differentiation. More mafic magmas erupted away from the volcano thanks to horizontal dyke propagation, whereas differentiated magmas erupted on the main edifice (Pinel and Jaupart, 2004). Only a few highly differentiated lava flows and dome could erupt inside the caldera or along the rim, and a high proportion of more basic lava flows were erupted outside the main edifice, as observed in the Payun Matru and Los Volcanes fields.

On the chondrite-normalized rare earth element patterns (Fig. 6c) and spider diagrams (Fig. 7c), samples of the Group G1, including the ignimbrite (88 AA, 94T1 and 94T2) and the caldera inner wall (94AH1), have strikingly identical patterns. This could suggest that magma did not have enough time to evolve between the last stage of the shield construction and the ignimbrite eruption. Such eruptions could occur when the magma has evolved into highly differentiated stages and became gas-saturated, so that the pressure inside the magma chamber caused a catastrophic eruption (Lipman, 1997). Alternatively, explosive eruptions can occur when a hot basaltic magma ascents and reaches a colder andesitic magma chamber and could induce magma mixing and the destabilization of the reservoir triggering the eruption (Lipman, 1997). Here, the fact that the ignimbrite samples have exactly the same geochemical signature and that there is no petrographic evidence for magma mixing allow us to propose that the depressurization of the reservoir has a tectonic rather than a magmatic origin.

Finally, we can infer that the magmatic evolution of Payun Matru volcanic field is linked to the tectonic setting at a regional scale. Its particular location into a back-arc domain could explain the fact that both basaltic lava flows and highly differentiated ignimbrite related to a caldera-forming eruption were erupted together in the same time frame.

6. Conclusions

The rocks studied here are related to the subduction of the Nazca plate beneath South America plate. Nevertheless, their back-arc location, under a thinned continental lithosphere, provides them with intraplate signatures. Such signatures could be emphasized by the influx of asthenosphere during and after the steepening of the slab, as previously suggested (e.g., Kay et al., 2006).

Based on 14 new K–Ar ages ranging from 285 ± 5 to 7 ± 1 ka and on 31 whole-rock major and trace element analyses, the history of the Payun Matru volcanic complex is now relatively well constrained. Our data outline the temporal relationship between basic and evolved magmas erupted in this complex. While a basaltic field was constructed over at least 3000 km^2, intermediate magma erupted rapidly, with an extrusion rate of about 4×10^{-3} km^3 yr^{-1}, to build the Payun Volcano at about 265 ± 5 ka. To the north, Payun Matru volcano started its edification with massive and thick evolved lavas before 168 ± 4 ka. Differentiation by crystal fractionation, associated with regional extension caused the sudden depressurization of the magma chamber and the emission of a large volume pyroclastic flow. This was related to the summit caldera collapse marking a drastic change of eruptive dynamism. Along the caldera rim, post-caldera activity took place, as well as on the external slopes and within the depression. Basalts did not erupt at the level of the Payun Matru volcano probably because of the edifice load. They were rather emitted in its vicinity along pre-existing EW trending fractures into strombolian and effusive eruptions. Finally, we have shown that the coeval eruption of basic and highly evolved lavas is still an ongoing process, with very young (less than 10 ka old) products emitted on Los Volcanes field as basaltic flows and strombolian cones, and on the Payun Matru volcano as trachyte lava flows.

Acknowledgements

The authors wish to thank the two anonymous reviewers and the editor Reynaldo Charrier for their useful comments that improved the manuscript. We thank Pierre Lahitte who contributed to GIS studies and volumes calculations. A. Hildenbrand, G. Delpech, R. Gertisser and S. Charbonnier are greatly acknowledged for their comments and suggestions. Many thanks to J. Carlut and D.

Winocur for help during sampling. Funding was obtained from INSU CNRS DyETI program. This is LGMT contribution No. 83.

References

Arana Saavedra, V., Aparicio, A., Bellido, F., Garcia Gacho, L., Viramonte, J., 1984. El volcanismo reciente de la vertiente oriental de los Andes entre los 34° y 37° de latitud sur (Provincia de Mendoza). In: Noveso Congreso Geologico Argentino, Bariloche, pp. 492–503.

Bermudez, A., Delpino, D., Frey, F., Saal, A., 1993. Los Basaltos de retroarco extraandinos. In: Ramos, V.A. (Ed.), XII Congreso Geologico Argentino y II Congreso de Exploracion de Hidrocarburos. Geologia y Recursos Naturales de Mendoza, Mendoza, pp. 161–172.

Bertotto, G.W., Bjerg, E.A., Cingolani, C.A., 2006. Hawaiian and Strombolian style monogenetic volcanism in the extra-andean domain of central-west Argentina. Journal of Volcanology and Geothermal Research 158 (3–4), 430–444.

Carignan, J., Hild, P., Mevelle, G., Morel, J., Yeghicheyan, D., 2001. Routine analyses of trace elements in geological samples using flow injection and low pressure on-line liquid chromatography coupled to ICP-MS: a study of reference materials BR, DR-N, UB-N, AN-G and GH. Geostandard Newsletter: the Journal of Geostandards and Geoanalysis 25 (2–3), 187–198.

Cassignol, C., Gillot, P.-Y., 1982. Range and effectiveness of unspiked potassium–argon dating: experimental groundwork and applications. In: Odin, G.S. (Ed.), Numerical Dating in Stratigraphy. John Wiley & Sons, pp. 159–179 (Chapter 9).

Davidson, J., de Silva, S., 2000. Composite volcanoes. In: Sigurdsson (Ed.), Encyclopedia of Volcanoes. Academic Press, pp. 663–681.

de Silva, S., Gosnold, W.D., 2007. Episodic construction of batholiths: insights from the spatiotemporal development of an ignimbrite flare-up. Journal of Volcanology and Geothermal Research 167, 320–335.

Delpino, D., 1993. Fue el sur mendocino similar a Hawaii? Evidencias del pasado para entender el presente. Malargue, Mendoza.

Folguera, A., Ramos, V.A., Zapata, T., Spagnuolo, M., Miranda, F., 2005. Pliocene to quaternary retro-arc extension in the Andes at 35°–37°30′S. In: 6th International Symposium on Andean Geodynamics (ISAG 2005), Barcelona, pp. 277–279.

Gillot, P.-Y., Cornette, Y., 1986. The Cassignol technique for potassium–argon dating, precision and accuracy: examples from the late Pleistocene to recent volcanism from southern Italy. Chemical Geology (Isotope Geoscience Section) 59, 205–222.

Gillot, P.-Y., Cornette, Y., Max, N., Floris, B., 1992. Two reference materials, trachytes MDO-G and ISH-G, for argon dating (K–Ar and $^{40}Ar/^{39}Ar$) of Pleistocene and holocene rocks. Geostandards Newsletter 16 (1), 55–60.

Gonzales Diaz, E., 1970. Rasgos morphologicos del Area Volcanica del Cerro volcan Payun Matru, Opera Lilloana XX.

Gonzales Diaz, E., 1972. Descripcion geologica de la Hoja 30d, Payun Matru, Provincia de Mendoza. Carta geologico-economica de la Republica Argentina, Escala 1:200,000, Buenos Aires.

Govindaraju, K., Mevelle, G., 1987. Fully automated dissolution and separation methods for inductively coupled plasma atomic emission spectrometry rock analysis. Application to the determination of Rare Earth Elements. Journal of Analytical Atomic Spectrometry 2, 615–621.

Govindaraju, K., Potts, P.J., 1994. 1994 report on Whin sill doleroite WS-E from England and Pitscurrie microgabbro PM-S from Scotland: assessment by one hundred and four international laboratories. Geostandard Newsletter: The Journal of Geostandards and Geoanalysis 18 (2), 211–300.

Gripp, A.E., Gordon, R.G., 2002. Young tracks of hotspots and current plate velocities. Geophysical Journal International 150, 321–361.

Inbar, M., Risso, C., 2001a. Holocene yardangs in volcanic terrains in the southern Andes, Argentina. Earth Surface Processes and Landforms 26 (6), 657–666.

Inbar, M., Risso, C., 2001b. A morphological and morphometric analysis of a high density cinder cone volcanic field – Payun Matru, South-Central Andes, Argentina. Zeitschrift fur Geomorphologie 45 (3), 321–343.

James, D.E., Sacks, I.S., 1999. Cenozoic formation of the Central Andes: a geophysical perspective. In: Skinner, B.J. (Ed.), Geology and Ore Deposits of the Central Andes. Society of Economic Geologists, pp. 1–22.

Kay, S.M., 2005. Tertiary to recent evolution of andean arc and back-arc magmas between 36°S and 38°S and evidence for Miocene shallowing of the Nazca plate under the Neuquén basin. In: 6th International Symposium on Andean Geodynamics (ISAG 2005), Barcelona, pp. 420–423.

Kay, S.M., Mpodozis, C., 2002. Magmatism as a probe to the Neogene shallowing of the Nazca plate beneath the modern Chilean flat-slab. Journal of South American Earth Sciences 15, 39–57.

Kay, S.M., Gorring, M.L., Ramos, V.A., 2004. Magmatic sources, setting and causes of Eocene to recent Patagonian plateau magmatism (36°S to 52°S latitude). Revista de la Asociacion Geologica Argentina 59 (4), 556–568.

Kay, S.M., Godoy, E., Kurtz, A., 2005. Episodic arc migration, crustal thickening, subduction erosion and magmatism in the South-central Andes. GSA Bulletin 117 (1/2), 67–88.

Kay, S.M., Burns, W.M., Copeland, P., Mancilla, O., 2006. Upper Cretaceous to Holocene magmatism and evidence for transient Miocene shallowing of the Andean subduction zone under the northern Neuquén basin. In: Ramos, S.M.K.a.V.A. (Ed.), Evolution of an Andean margin: a tectonic and magmatic view from the Andes to the Neuquén basin (35–39°S lat). The Geological Society of America, pp. 19–60/359.

Le Bas, M.J., Le Maitre, R.W., Streckeisen, A., Zanettin, B., 1986. A chemical classification of volcanic rocks based on the total alkali–silica diagram. Journal of Petrology 27 (Part 3), 745–750.

Lipman, P.W., 1997. Subsidence of ash-flow calderas: relation to caldera size and magma-chamber geometry. Bulletin of Volcanology 59, 198–218.

Munoz, J., Troncoso, R., Duhart, P., Crignola, P., Farmer, L., Stern, C., 2000. The relation of the mid-tertiary coastal magmatic belt in south-central Chile to late Oligocene increase in plate convergence rate. Revista Geologica de Chile 27 (2), 177–203.

Odin, G.S., and 35 collabotators, 1982. Interlaboratory standards for dating purposes. In: Odin, G.S. (Ed.), Numerical Dating in Stratigraphy, pp. 123–150.

Pasquarè, G., Bistacchi, A., Francalanci, L., Bertotto, G.W., Boari, E., Massironi, M., Rossotti, A., 2008. Very long pahoehoe inflated basaltic lava flows in the Payenia volcanic province (Mendoza and La Pampa, Argentina). Revista de la Asociación Geológica Argentina 63 (1), 131–149.

Peccerillo, A., Taylor, S.R., 1976. Geochemistry of Eocene calc-alkaline volcanic rocks of the Kastamonu area, Northern Turkey. Contributions to Mineralogy and Petrology 58, 63–81.

Pinel, V., Jaupart, C., 2000. The effect of edifice load on magma ascent beneath a volcano. Philosophical Transactions of the Royal Society of London. Series A, Mathematical and Physical Sciences 358, 1515–1532.

Pinel, V., Jaupart, C., 2004. Magma storage and horizontal dyke injection beneath a volcanic edifice. Earth and Planetary Science Letters 221, 245–262.

Quidelleur, X., Gillot, P.-Y., Soler, V., Lefèvre, J.-C., 2001. K/Ar dating extended into the last millennium: application to the youngest effusive episode of the Teide volcano (Spain). Geophysical Research Letters 28 (16), 3067–3070.

Quidelleur, X., Carlut, J., Tchilinguirian, P., Germa, A., Gillot, P.-Y., 2009. Paleomagnetic directions from mid-latitude sites in the southern hemisphere (Argentina): contribution to time averaged field models. Physics of the Earth and Planetary Interiors 172, 199–209.

Ramos, V.A., Folguera, A., 2005. Structural and magmatic responses to steepening of a flat subduction, southern Mendoza, Argentina. In: 6th International Symposium on Andean Geodynamics (ISAG 2005), Barcelona, pp. 592–595.

Ramos, V.A., Kay, S.M., 2006. Overview of the tectonic evolution of the southern central Andes of Mendoza and Neuquén (35°–39° latitude). In: Ramos, S.M.K.a.V.A. (Ed.), Evolution of an Andean Margin: a Tectonic and Magmatic View from the Andes to the Neuquén Basin (35–39°S lat). The Geological Society of America, pp. 1–17.

Risso, C., Nemeth, K., Combina, A.M., Nullo, F., Drosina, M., 2008. The role of phreatomagmatism in a Plio-Pleistocene high-density scoria cone field: Llancanelo volcanic field (Mendoza), Argentina. Journal of Volcanology and Geothermal Research 169 (1–2), 61–86.

Sarbas, B., Nohl, U., 2008. The GEOROC database as a part of a growing geoinformatics network. In: Brady, S.R., Sinha, A.K., Gundersen, L.C. (Eds.), Geoinformatics 2008 – Data to Knowledge, Proceedings: US Geological Survey Scientific Investigation Report 2008-5172, pp. 42–43.

Singer, B., Thompson, R.A., Dungan, M., Feeley, T.C., Nelson, S.T., Pickens, J.C., Brown, L.L., Wulff, A.W., Davidson, J., Metzger, J., 1997. Volcanism and erosion during the past 930 ky at the Tatara-San Pedro complex, Chilean Andes. GSA Bulletin 109 (2), 127–142.

Steiger, R.H., Jäger, E., 1977. Subcommission on geochronology: convention on the use of decay constants in geo and cosmochronology. Earth and Planetary Science Letters 36 (3), 359–362.

Stern, C., Frey, F., Futa, K., Zartman, R., Peng, Z., Kyser, T., 1990. Trace-element and Sr, Nd, Pb, and O isotopic composition of Pliocene ans Quaternary alkali basalts of the Patagonian Plateau lavas of southernmost South America. Contributions to Mineralogy and Petrology 104, 294–308.

Sun, S.S., McDonough, W.F., 1989. Chemical and isotopic systematics of oceanic basalts: implications for mantle composition and processes. In: Saunders, A.D., Norry, M.J. (Eds.), Magmatism in Ocean Basins. Geological Society, London, pp. 313–345.

White, S.M., Crisp, J.A., Spera, F.J., 2006. Long-term volumetric eruption rates and magma budgets. Geochemistry Geophysics Geosystems 7 (3), 20.